

SHORT-TERM PHOTOVOLTAIC POWER FORECASTING BASED ON ARTIFICIAL NEURAL NETWORKS: A NUMERICAL WEATHER PREDICTION-FREE APPROACH

Spyros Theocharides^{1,*}, George Makrides¹, Marios Theristis¹, Florencia Almonacid², Eduardo F. Fernández²
and George E. Georghiou¹

¹PV Technology Laboratory, FOSS Research Centre for Sustainable Energy, Department of Electrical and Computer Engineering, University of Cyprus, Nicosia, 1678, Cyprus

²Centre for Advanced Studies on Energy and Environment (CEAEMA), IDEA Solar Energy Research Group, Electronics and Automation Engineering Department, University of Jaén, Jaén, 23071, Spain

*corresponding author email: theocharidis.spyros@ucy.ac.cy

ABSTRACT: The increased penetration of photovoltaic (PV) systems introduce new challenges for the stability of electricity grids. In this scope, a machine learning technique utilising artificial neural networks (ANN) was implemented to forecast the hour-ahead (HA) PV power production without the utilisation of numerical weather prediction (NWP) models. Instead, historical PV operational and meteorological data-sets were used for the training and validation stages of the model to calculate HA PV power generation data-sets for time $t + 1h$ while the model input parameters (weather measurements) were applied for time t . The best-performing model comprised of four input parameters (in-plane global irradiance (G_i), ambient temperature (T_{amb}), elevation angle (ALS), azimuth angle (AzS)), a single hidden layer and 22 hidden neurons. Additionally, the results obtained over a test set period of 55 days demonstrated that accurate HA forecasts could be achieved without incorporating NWP since a daily-normalised root mean square error (nRMSE) of 3.63% was achieved. Finally, the model performed very well during clear sky days with a nRMSE close to 1% whereas 57% of all days demonstrated a nRMSE below 5%.

Keywords: artificial neural networks, forecasting, photovoltaic, power.

1 INTRODUCTION

Accurate PV production forecasting can mitigate the power quality effects posed by large shares of distributed systems through active grid management and is, therefore, an important feature that can assist utilities and plant operators in the direction of energy management and dispatchability planning. More specifically, short-term PV production forecasts (intra-hour) are necessary for power ramp and voltage flicker prediction as well as control operations and dispatch management. On the other hand, mid-term PV production forecasting (intra-day and day-ahead) is used for load consumption and production monitoring to control voltage and frequency levels and reduce secondary reserve.

During the last decades, electricity system operation has been upgraded involving PV production forecasts and most commonly adopted PV production forecasting approaches are based on time series analysis techniques [1]. In addition, parametric models for PV production forecasting have already been developed [2], [3] but their ability to forecast the power output of PV systems is not a straightforward process since accurate knowledge of system characteristics and behaviour should be provided. Therefore, a huge share of research is devoted to the development of more sophisticated and flexible prediction techniques using non-parametric models based on machine learning algorithms [4]–[9]. In order to train a PV power forecasting model with identical data, weather classification and machine learning techniques may be performed [10], [11]. Moreover, joint models comprised of combination of features of a physical model combined with artificial neural networks (ANNs) were presented elsewhere [7], [12]. Although a significant number of PV power forecasting tools have been developed, the challenge to provide a global and validated (against large scale data-sets) model for different PV remains unsolved. Additionally, to improve the accuracy of the power prediction of PV systems, adaptive methods that can capture system information and behaviour without the need of datasheet and

installation parameters must be employed. This is crucial because a large proportion of PV systems includes decentralized rooftop installations where knowledge of system information is not always available.

Furthermore, the system's behaviour can be estimated by processing recent PV operational data-sets using the classical approach of the feedforward neural network (FFNN). This method was inspired by the method of biological neurons and is the simplest type of ANNs. It is a popular and powerful machine learning algorithm widely used in other fields for both prediction and classification purposes. The classical approach of the FFNN with an input, a hidden and an output layer of linear and non-linear activation functions can be viewed as a convenient way to predict the power output of PV systems. FFNN can be trained to develop relational weighted chains between internal nodes to overcome the limitations of traditional methods to solve complex problems, which can be modelled through a supervised learning technique based on historical data. Because of this chain of relationships, theoretically, multi-layered neural networks can be universal approximators and have tremendous potential to perform any nonlinear mapping through a learning process based on historical time-series [13]. In addition, ANNs are efficient for online training due to their capability of reflecting the information of new instances on a model by changing the weight values only.

Another approach is to utilise Numerical Weather Prediction (NWP) models to forecast weather variables [3], [14]–[16]. NWP models deliberate the atmosphere as a fluid thus the concept of weather forecasts is to parametrise the state of the fluid at a certain time (t) by utilising the fluid- and thermo-dynamic equations to forecast the state of the fluid at time ($t + n$) [17]–[19]. The utilisation of mathematical equations and models to simulate the atmosphere are not accurate, thus the NWP methods are associated with forecasting errors and biases [20], [21].

In this work, a NWP free methodology for hour-ahead (HA) PV power production forecasting utilising

data-driven machine learning models and specifically ANNs is proposed in this study. One-year data from a reference poly-crystalline silicon (poly-c-Si) PV system in Cyprus were used for training and testing the model and the forecasting performance results showed that the application of this method improves the HA PV production forecasting accuracy.

2 EXPERIMENTAL SETUP

2.1. Outdoor test facility description

The outdoor test facility of the University of Cyprus includes a fixed plane infrastructure for outdoor performance assessments at both the module and system level. The installed poly-c-Si system was mounted in a portrait arrangement on aluminium mountings, at the optimum annual energy yield plane-of-array (POA) angle for Cyprus of 27.5° .

The PV system was connected to a data-acquisition platform, used for the monitoring and storage of meteorological and PV operational data. The performance of the system and the prevailing meteorological conditions were recorded according to the requirements set by the IEC 61724 [22]. Specifically, the irradiance and meteorological measurements include the in-plane global irradiance (G_t), relative humidity (RH), wind direction (W_a), wind speed (W_s) and ambient temperature (T_{amb}). The PV system operational measurements include the maximum power current (I_{mp}), voltage (V_{mp}) and power (P_{mp}), as measured at the output of the PV array (DC side) [23], [24].

2.2 PV system description

The PV system comprises of five poly-c-Si PV modules. The modules of the system are connected in series to form a PV string at the input of a string inverter. The main technical specifications of the test PV system are summarised in Table I.

Table I: Installed PV system technical characteristics.

Technical characteristic	Parameter
Modules	$5 \times$ poly-c-Si
System power (datasheet)	1365 W _p
Installation date	01/06/2015
Efficiency	14.40%

3 METHODOLOGY

The HA PV power production forecasting model was based on a FFNN that employed recent historical data-sets of a reference PV system, as the training parameters of the model. The best-performing neural network was chosen through a series of validation tests performed by identifying optimum combinations of input parameters, sizes and hyper (architectural) parameters of the model (optimal hidden layers, neurons, iterations and learning function). The historical PV operational and meteorological data-sets were used for both the training and validation stages of the model. For each model, the training step yielded the respective HA PV power (output parameter) for time $t + 1h$ while the model input parameters (weather measurements) were applied for time t . The aim of the training step was to develop a model which is capable of accurately forecasts the power generation for time $t + 1h$, based on the relationships

established between the weather measurements of time t (without incorporating forecasted weather data) and the actual output PV produced power of the reference system at time $t + 1h$.

In particular, the annual historical data-sets of the reference system and prevailing weather conditions were divided into three subsets, the training, validation and testing set. The training and validation sets were utilised in order to implement the best-performing model, by varying the training period from 30% to 70% of the actual data-set. The model inputs included the meteorological parameters in addition to the solar elevation angle (AlS) and solar azimuth angle (AzS) that were calculated using solar position algorithms [25], [26]. Additionally, the hyper parameters of the neural network were tested by varying the number of hidden neurons, layers, iterations and learning function. The validation set was employed in order to evaluate the performance of the various neural network models and therefore identify the best performing model, while the test set was applied in order to yield forecasting results for the developed model. The complete methodological steps followed for the development of the short-term HA PV power production forecasting model are exhibited in Fig. 1 and Eq. (1).

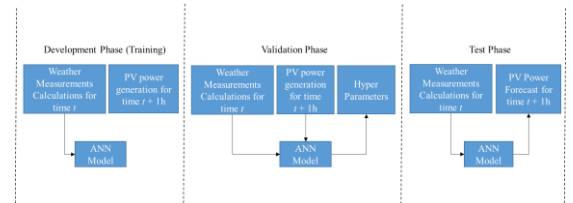


Figure 1: Training, validation and testing phases of the short-term HA PV power production forecasting model.

$$P_{DC}(t+1) = G_t(t) + T_{amb}(t) + \dots \quad (1)$$

Where $P_{DC}(t + 1)$ is the power for time $t + 1$, $G_t(t)$, $T_{amb}(t)$, \dots , are the weather measurements for time t .

3.1 Neural network

A Bayesian Regularization Neural Network (BRNN) is essentially a simple Multi-Layer Perceptron (MLP), in which a Bayesian regularization has been applied to its training function. The proposed model is given by Eq. (2) [27], [28]:

$$y_i = g(x_i) + e_i = \sum_{k=1}^9 w_k g_k(b_k + \sum_{j=1}^p x_j \beta_j^{[k]}) + e_i, i = 1, \dots, n \quad (2)$$

where $e_i \sim N(0, \sigma^2 e)$, s is the number of neurons, w_k is the weight of the k -th neuron, b_k is a bias for the k -th neuron, $\beta_j^{[k]}$ is the weight of the j -th input to the net, and $g_k(\cdot)$ is the activation function:

$$g_k(x) = \frac{\exp(2x) - 1}{\exp(2x) + 1} \quad (3)$$

The model will minimise according to Eq. (4) [27], [28]

$$F = \beta E_D + \alpha E_W \quad (4)$$

where E_D is the error of sum squares, E_W is the sum of squares of network parameters (weights and biases). E_W

is the sum of squares of network parameters (weights and biases), β and α are the dispersion parameters for weights and biases.

The regularisation term applied was the squared sum of the weights of the neural network [29]:

$$\varepsilon_T = \beta \varepsilon_D + \alpha \varepsilon_R = \frac{\beta}{2} \sum_{k=1}^N (y_k - t_k)^2 + \frac{\alpha}{2} \sum_{i=2}^M w_i^2 \quad (5)$$

where α and β are coefficients assigned to each term. The second term in Eq. (5) is called weight decay, as it ensures that the weights of the network do not exceed the total error of the network.

After the data were fed into the network, the density function for the weights can be updated according to Bayes' rule [28]:

$$P(w|D, \alpha, \beta, M) = \frac{P(D|w, \beta, M)P(w|\alpha, M)}{P(D|\alpha, \beta, M)} \quad (6)$$

where D represents the data-set, M the model used for the Neural Network and w is the vector of neural network's weights. $P(w|\alpha, M)$ represents the values of weights prior to the data-set input. $P(D|w, \beta, M)$ is the probability of the data occurring based on the weights. $P(D|\alpha, \beta, M)$ is a normalisation factor, which ensures that the total summation of the probability is one.

In addition, the regularisation term is used to prevent overfitting, by controlling the effective complexity of the neural network. The regularisation of the designed networks in this study was performed by adding a penalty equal to the L2-norm of the weights, in order to reduce the value of the weights by the same factor.

3.2 Model architecture

The acquired annual data-set of the PV system was divided into three different sets in order to determine the optimal parameters for the neural network. The annual data-set was separated into the train, validation and test set with the 70:15:15% portion approach [30]. The 70:15:15% data split portion was selected in order to include systematic information for the training but to also preserve sufficient data-points for validation and testing. The data splitting techniques involved the partitioning of data into an explicit training set used to develop the model, the validation set used to tune the parameters of the model and the test set necessary to evaluate the model performance on unseen data. The training, validation and testing set, comprised of the model inputs which included the measurements of G_i , T_{amb} , RH , W_s , W_a and the calculated parameters of AzS and AIS . Finally, the DC P_{mp} was the output parameter of the model.

In order to achieve optimal forecasting performance, different input feature combinations and hidden layer topologies (number of hidden units) were investigated while training the network models. The initially designed FFNN, which was subsequently used in the tuning process comprised of two inputs (G_i , T_{amb}), four hidden nodes and an output layer (P_{mp}) (see Fig. 2). The optimal model parameters were identified by comparing the performance of the developed models based on the training and validation sets. Re-iteration of the process (epochs) was performed until the results from the network became acceptable, indicating low performance

error while avoiding over-training the network, that may result in over-fitting.

Lastly, the tuned networks were then evaluated by feeding the test set input variables and assessing the actual measured power against the predicted power according to some performance assessment metrics (that will be discussed later).

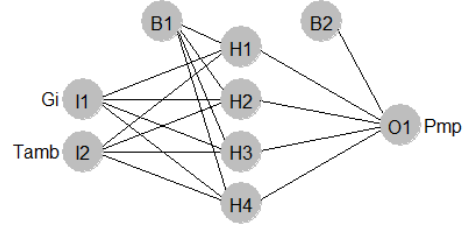


Figure 2: Network interconnection diagram (NID) of a FFNN.

3.3 Model performance assessment

The forecasting performance accuracy was assessed based on several predefined metrics when the test set was applied to the developed algorithms. The metrics commonly used in PV production forecasting applications include the mean absolute error (MAE), mean absolute percentage error (MAPE), root mean square error (RMSE) and normalised RMSE (nRMSE) to the nominal PV system peak power:

$$MAE = \frac{1}{n} \times \sum_{i=1}^n |y_{actual,i} - y_{predicted,i}| \quad (7)$$

$$MAPE = \frac{100}{n} \times \sum_{i=1}^n \left| \frac{y_{actual,i} - y_{predicted,i}}{y_{actual,i}} \right| \quad (8)$$

$$MBE = \frac{100}{n} \times \sum_{i=1}^n \frac{y_{actual,i} - y_{predicted,i}}{y_{actual,i}} \quad (9)$$

$$RMSE = \sqrt{\frac{1}{n} \times \sum_{i=1}^n (y_{actual,i} - y_{predicted,i})^2} \quad (10)$$

$$nRMSE = \frac{100}{P_{nominal}} \times \sqrt{\frac{1}{n} \times \sum_{i=1}^n (y_{actual,i} - y_{predicted,i})^2} \quad (11)$$

where $y_{actual,i}$ and $y_{forecasted}$, is the actual and predicted power respectively, $P_{nominal}$ is the nominal peak power of the PV system (1365 W).

4 RESULTS

In order to establish an accurate HA PV power production forecasting model, it is necessary to analyse the sensitivity of the output on the input variables. For this purpose, the influence of each input parameter on the output power, was examined by calculating the Pearson Correlation Coefficient (PCC), which measures the direction and strength of the linear relationship between two variables. Table II summarises the results from the PCC between the investigated features.

Table II: Pearson Correlation Coefficient between PV power output and environmental factors under typical weather conditions.

	Pearson Correlation Coefficient
	Maximum Power, P_{mp}
Incident global irradiance, G_I	0.86
Sun elevation angle, AIS	0.77
Relative humidity, RH	-0.74
Ambient temperature, T_{amb}	-0.60
Wind direction, W_a	-0.10
Wind speed, W_s	0.10
Sun azimuth angle, AzS	-0.01

Intending to select only the highly linearly correlated input parameters, a threshold was set at the Pearson Coefficient; i.e. $|PCC| \geq 0.5$. The parameters complying with the set threshold level were the G_I , AIS , T_{amb} and RH . In order to achieve a model optimisation, different input parameter combinations at the input layer of each devised network were investigated comprising not only of the highly correlated parameters but also the remaining input parameters that exhibited non-linear behaviour. However, the highly correlated input parameters were expected to achieve high accuracy and feature importance. In addition, the number of hidden units was set to an empirical value between the total of the number of inputs and output layer nodes. Table III tabulates the validation results based on the nRMSE of the input feature analysis to the FFNN model.

Table III: Input feature parameter models and the corresponding nRMSE.

Input features	Hidden Layer Neurons	nRMSE (%)
G_I, T_{amb}	2	5.50
G_I, T_{amb}, AIS	3	5.27
G_I, T_{amb}, RH	3	5.68
G_I, T_{amb}, RH, AIS	4	5.33
$G_I, T_{amb}, W_{alpha}, W_s$	4	6.10
G_I, T_{amb}, AIS, AzS	4	4.60
G_I, T_{amb}, W_s, RH	4	5.13
$G_I, T_{amb}, AzS, AIS, W_a, W_s, RH$	7	5.77

The results clearly demonstrated that the optimum feature combination included all the input variables (G_I , T_{amb} , AzS , AIS), confirming that FFNNs could detect both the linear and non-linear behaviours among the input and output parameters. Varying the number of input features resulted in an nRMSE ranging from 6.10% to 4.60%, which highlights the robustness of neural networks.

To further improve the accuracy of the predictions of the optimal network, the effect of varying the number of hidden units on the prediction accuracy was also investigated. The results presented in Fig. 3, demonstrate that the nRMSE decreases with the increasing number of hidden units, in the case of the training set.

In particular, although the training set was improving by increasing the number of hidden neurons, the nRMSE of the validation set showed a different behaviour when the number of hidden neurons was increased beyond a certain number. The results presented in the plot showed that the best accuracy for the validation set was obtained when the selected number of hidden neurons was in the range of 22 to 25. To minimise the error and the noise of

the training phase more hidden units were utilised. However, to decrease the complexity of the model and prone to overfitting [31] the number of nodes was set to 22 in the hidden layer as an additional optimisation step, which yielded a nRMSE of 3.63%.

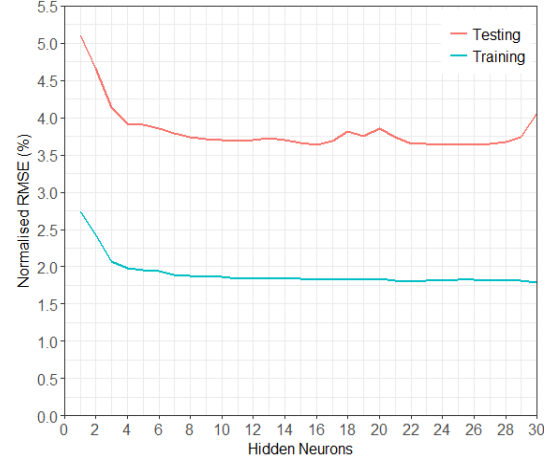


Figure 3: Daily nRMSE (%) against the number of neurons for both the training and validation sets using a single hidden layer.

At this stage, the neural network was designed by specifying the number of input variables and amount of hidden neurons. The optimal model therefore comprised of the input parameters of G_I , T_{amb} , AzS and AIS . The 70% of randomly selected samples and a single hidden layer with 22 neurons (see Fig. 4) developed the training set of the ANN model. Additionally Eq. (12) describes the best-performing model.

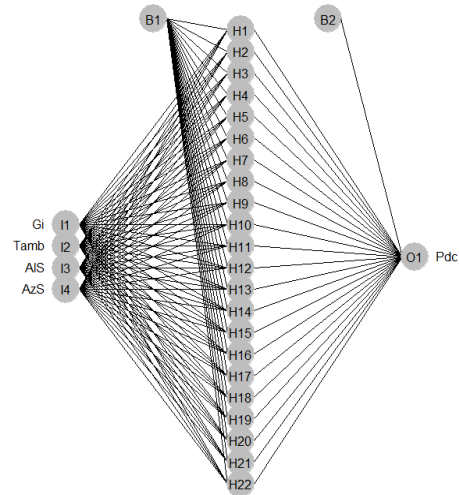


Figure 4: NID of the optimally designed FFNN.

$$P_{DC}(t+1) = G_I(t) + T_{amb}(t) + AIS(t) + AzS(t) \quad (12)$$

When the testing set data were applied to the model, the daily average nRMSE was 3.60%, while 57% of the days demonstrated a nRMSE below 5% (Fig. 5). Furthermore, when typical weekly data with both clear and overcast days were applied to the model it was found that the systematic behaviour of the PV system was captured (see Fig. 6a). Specifically, the error relative to the capacity of the system for all points during clear sky

was in most cases less than 0.1 W/Wp (see Fig. 6b).

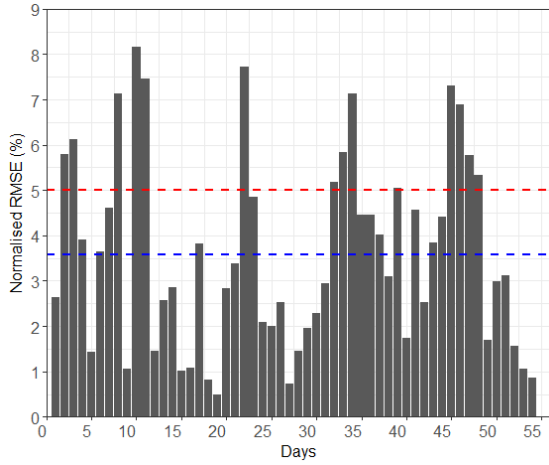


Figure 5: Daily nRMSE over the test set samples. The dashed blue line represents the daily nRMSE of 3.60% while the red dashed line demonstrates the 5% threshold.

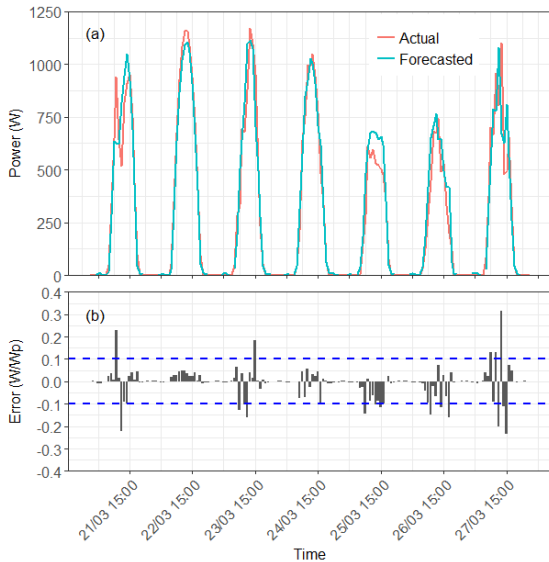


Figure 6: Plot of daily (a) Actual against HA PV power forecast and (b) Error relative to the capacity.

In addition, the MBE of the testing set was found to be 0.1%, indicating that there is no significant bias in the forecasts (neither an overestimation nor an underestimation of the forecasted P_{mp} , over the actual P_{mp}) (see Fig. 7).

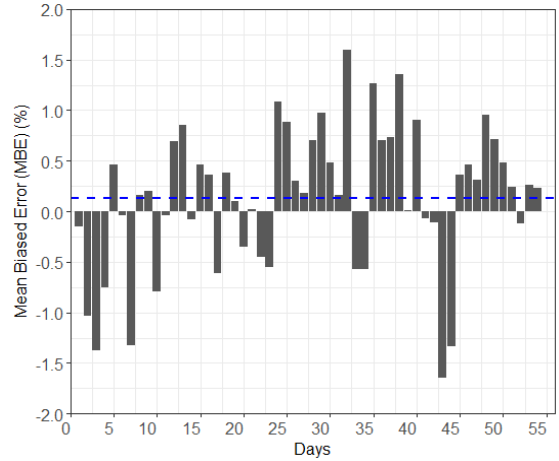


Figure 7: Daily forecasted bias error. The blue dashed line represents the MBE (~-0.1%).

5 CONCLUSION

Increased PV penetration requires agile forecasting techniques in order to ensure grid stability and dispatchability. For the development of an accurate ANN model, a procedure with subsequent stages of training and testing steps was followed and the devised ANNs were assessed by tuning their input features and network architecture. More specifically, a conventional FFNN was designed, whose parameters were estimated by a feedforward supervised learning process, trained using the BP technique and regularised by employing L2 regularisation. The final ANN comprised of 4 input parameters (G_t , T_{amb} , AzS , AIS), 22 hidden neurons and was trained with a random samples of 70:15:15% train, validation and test set approach.

The forecasting results demonstrated that the average daily nRMSE was 3.60% over the tests period and the model performed very well during clear sky days exhibiting a nRMSE close to 1% while the MBE was 0.15% indicating no biases between the forecasted and the actual power.

6 ACKNOWLEDGEMENT

This work was funded through the INFORPV project which is co-financed by the SOLAR-ERA.NET Transnational Calls of the European Union under the grant agreement number SOLAR-ERA.NET/1215/02.

7 REFERENCES

- [1] S. Pelland, J. Remund, J. Kleissl, T. Oozeki, and K. De Brabandere, "Photovoltaic and Solar Forecasting: State of the Art," *Int. Energy Agency Photovolt. Power Syst. Program. Rep. IEA PVPS T14*, pp. 1–40, 2013.
- [2] E. Lorenz, T. Scheidsteger, J. Hurka, D. Heinemann, and C. Kurz, "Regional PV power prediction for improved grid integration," *Prog. Photovoltaics Res. Appl.*, vol. 19, no. 7, pp. 757–771, 2011.

- [3] S. Pelland, G. Galanis, and G. Kallos, "Solar and photovoltaic forecasting through post-processing of the Global Environmental Multiscale numerical weather prediction model," *Prog. Photovoltaics Res. Appl.*, vol. 21, no. 3, pp. 284–296, 2013.
- [4] I. Ashraf and a Chandra, "Artificial neural network based models for forecasting electricity generation of grid connected solar PV power plant," *Int. J. Glob. Energy Issues*, vol. 21, no. 1, pp. 119–130, 2004.
- [5] D. Caputo, F. Grimaccia, M. Mussetta, and R. E. Zich, "Photovoltaic plants predictive model by means of ANN trained by a hybrid evolutionary algorithm," in *Proceedings of the International Joint Conference on Neural Networks*, 2010.
- [6] S. A. Kalogirou, "Applications of artificial neural-networks for energy systems," *Appl. Energy*, vol. 67, no. 1–2, pp. 17–35, 2000.
- [7] A. Gandelli, F. Grimaccia, S. Leva, M. Mussetta, and E. Ogliari, "Hybrid model analysis and validation for PV energy production forecasting," in *Proceedings of the International Joint Conference on Neural Networks*, 2014, pp. 1957–1962.
- [8] A. Mellit and A. M. Pavan, "A 24-h forecast of solar irradiance using artificial neural network: Application for performance prediction of a grid-connected PV plant at Trieste, Italy," *Sol. Energy*, vol. 84, no. 5, pp. 807–821, 2010.
- [9] F. Almonacid, P. J. Pérez-Higueras, E. F. Fernández, and L. Hontoria, "A methodology based on dynamic artificial neural network for short-term forecasting of the power output of a PV generator," *Energy Convers. Manag.*, vol. 85, pp. 389–398, 2014.
- [10] C. Chen, S. Duan, T. Cai, and B. Liu, "Online 24-h solar power forecasting based on weather type classification using artificial neural network," *Sol. Energy*, vol. 85, no. 11, pp. 2856–2870, 2011.
- [11] J. Shi, W. J. Lee, Y. Liu, Y. Yang, and P. Wang, "Forecasting power output of photovoltaic system based on weather classification and support vector machine," in *Conference Record - IAS Annual Meeting (IEEE Industry Applications Society)*, 2011.
- [12] A. Dolara, F. Grimaccia, S. Leva, M. Mussetta, and E. Ogliari, "A physical hybrid artificial neural network for short term forecasting of PV plant power output," *Energies*, vol. 8, no. 2, pp. 1138–1153, 2015.
- [13] M. P. Almeida, M. Muñoz, I. de la Parra, O. P. Lamigueiro, and L. N. Fernández, "Comparative study of nonparametric and parametric PV models to forecast AC power output of PV plants," in *EU PVSEC Proceedings*, 2015, pp. 2230–2234.
- [14] S. E. Haupt *et al.*, "Building the Sun4Cast System: Improvements in Solar Power Forecasting," *Bull. Am. Meteorol. Soc.*, vol. 99, no. 1, pp. 121–136, 2018.
- [15] D. P. Larson, L. Nonnenmacher, and C. F. M. Coimbra, "Day-ahead forecasting of solar power output from photovoltaic plants in the American Southwest," *Renew. Energy*, vol. 91, pp. 11–20, 2016.
- [16] X. Sun and T. Zhang, "Solar Power Prediction in Smart Grid Based on NWP Data and an Improved Boosting Method," in *Proceedings - 1st IEEE International Conference on Energy Internet, ICEI 2017*, 2017, pp. 89–94.
- [17] P. Lynch, "The origins of computer weather prediction and climate modeling," *J. Comput. Phys.*, vol. 227, no. 7, pp. 3431–3444, 2008.
- [18] L. F. Richardson, *Weather prediction by numerical process, second edition*. 2007.
- [19] R. Kimura, "Numerical weather prediction," *J. Wind Eng. Ind. Aerodyn.*, vol. 90, no. 12–15, pp. 1403–1414, 2002.
- [20] H.-L. Xue, X.-S. Shen, and J.-F. Chou, "A forecast error correction method in numerical weather prediction by using recent multiple-time evolution data," *Adv. Atmos. Sci.*, vol. 30, no. 5, pp. 1249–1259, 2013.
- [21] L. Gao, H.-L. Ren, J.-P. Li, and J.-F. Chou, "Analogue correction method of errors and its application to numerical weather prediction," *Chinese Phys.*, vol. 15, no. 4, pp. 882–889, 2006.
- [22] British Standard, "IEC 61724:1998. Photovoltaic system performance monitoring — Guidelines for measurement, data exchange and analysis," p. 20, 1998.
- [23] G. Makrides, B. Zinsser, M. Norton, G. E. Georghiou, M. Schubert, and J. H. Werner, "Potential of photovoltaic systems in countries with high solar irradiation," *Renewable and Sustainable Energy Reviews*, vol. 14, no. 2, pp. 754–762, 2010.
- [24] G. Makrides, B. Zinsser, M. Schubert, and G. E. Georghiou, "Energy yield prediction errors and uncertainties of different photovoltaic models," *Prog. Photovoltaics Res. Appl.*, vol. 21, no. 4, pp. 500–516, 2013.
- [25] I. Reda and A. Andreas, "Solar position algorithm for solar radiation applications," *Sol. Energy*, vol. 76, no. 5, pp. 577–589, 2004.
- [26] NREL, "Solar Position Algorithm (SPA) Source Code," *NREL Renewable Resource Data Center (RReDC)*, 2008. [Online]. Available: <http://rredc.nrel.gov/solar/codesandalgorithms/spa/>.
- [27] D. E. Rumelhart, G. E. Hinton, and R. J. Williams, "Learning representations by back-propagating errors," *Nature*, vol. 323, no. 6088, pp. 533–536, 1986.
- [28] D. J. C. MacKay, "Bayesian Interpolation," *Neural Comput.*, vol. 4, no. 3, pp. 415–447, 1992.
- [29] F. Dan Foresee and M. T. Hagan, "Gauss-Newton approximation to bayesian learning," in *IEEE International Conference on Neural Networks - Conference Proceedings*, 1997, vol. 3, pp. 1930–1935.
- [30] S. Theocharides, G. Makrides, V. Venizelou, P. Kaimakis, and G. E. Georghiou, "Pv Production Forecasting Model Based on Artificial Neural Networks (Ann)," *33rd Eur. Photovolt. Sol. Energy Conf.*, pp. 1830–1894, 2017.
- [31] K. P. Burnham and D. R. Anderson, "Model Selection and Multimodel Inference," *Model Sel. Multimodel Inference*, pp. 49–97, 2004.